

# Topology Optimization for Maximum Daily Solar Radiation for a Large-Scale Non-tracking Heliostat Solar Reflector Using CFD Analysis



Sunny J. Shiyal, Bamaniya Jayesh Pravinbhai, Guru Bachan Satsangi, and Amit R. Patel

**Abstract** The present research work proposes a method to optimize the geometrical parameters of a large-scale heliostat reflector using CFD analysis. The use of heliostat reflectors in solar cookers is well established because of its low-cost production. Determining the best configuration of a fixed shape of inverted frustum of a square pyramid reflector is very helpful as it can avoid the tracking of reflector. The reflector height and dimensions of sides of the top surface are kept constant which are 1.75 and  $5 \times 5 \text{ m}^2$ , respectively. Results are obtained by varying the dimensions of the bottom sides of the reflector by 5%. All 32 combinations are tested for a time interval of 15 min considering daily radiation data for the time period starting from 0900 to 1700 h. To analyze the effect of these varying parameters, total daily radiation heat flux at the top and base is calculated, and a dimensionless concentration factor is calculated to get the topology optimization. Two dimensionless parameters are identified, viz., height-to-base ratio and area ratio of top to bottom surface, the values of which are 0.7 and 2. These dimensionless geometrical parameters can be utilized to manufacture heliostat solar reflectors.

**Keywords** Radiation · Heliostat reflector · CFD · Ansys · Fluent

## Nomenclature

$T$	Thickness of the reflector [m]
$A_b$	Area of the base [ $\text{m}^2$ ]
$A_t$	Area of the top [ $\text{m}^2$ ]
$BS$	Bottom side of the reflector [m]
$C_p$	Heat capacity at constant pressure [J/mK]

---

S. J. Shiyal · B. J. Pravinbhai · G. B. Satsangi · A. R. Patel (✉)

Department of Mechanical Engineering, Faculty of Technology and Engineering, The Maharaja Sayajirao University of Baroda, Vadodara, Gujarat, India

e-mail: [a.r.patel-med@msubaroda.ac.in](mailto:a.r.patel-med@msubaroda.ac.in)

$H$	Height of the configuration [m]
$H$	Height of the reflector [m]
$K$	Thermal conductivity [ $\text{W}/\text{m}^2\text{K}$ ]
$p_{atm}$	Atmospheric pressure [bar]
$T_{atm}$	Atmospheric temperature [K]
$t_b$	Thickness of the base [m]
$TS$	Top side of the reflector [m]
$W_b$	Width at the base/bottom [m]
$\varepsilon$	Emissivity of the reflector [-]
$W_t$	Width at the top [m]
$P$	Density [ $\text{kg}/\text{m}^3$ ]

## 1 Introduction

India is the world's third largest renewable energy producer with 38% of energy capacity installed in year 2020 coming from renewable sources [1]. In November 2021, India had an installed renewable energy capacity of 150 GW in which 48.55 GW (32.36%) was from solar itself [2]. For achieving sustainable development, the use of renewable energy is necessary. Specific technologies have been intensively used and invented in recent times in the area of solar energy utilization. These methods are not as effective as conventional energy sources due to its efficiency issues. For that reason, industries related to solar energy tries to invent the cost-effective manufacturing, installation, and maintenance methods. Solar thermal energy has been utilized in different applications varying from cooking, drying to electricity generation. The basic principle used for solar energy utilization is to capture the maximum solar radiation emitted by the sun. For this, many researchers have proposed various techniques. In one of such applications, the use of heliostat reflector is used. The concentration of solar radiation by means of a number of heliostats distributed in the horizontal plane onto a receiver mounted on a tower is known as a central receiver system or tower system. The concentration system of this kind is considered to be the most useful for large-scale solar thermal processes such as electric power generation [3].

The efficiency of the heliostat reflector largely depends on the geometrical parameters or its configuration. Several attempts are made by researchers to optimize the dimensions of heliostat reflectors. Riaz stated in his research that a major feature of the ideal solar plant characteristics is their unique dependency on just two parameters: the sun Zenith angle  $\theta_s$  (i.e., the time of the day) and the size of concentrator [4]. This is because the reflectors are already aligned to the path traced by the sun for a particular day. Takemaro calculated solar concentrations theoretically by central receiver systems for various values of obliquity of the incident radiation for plane heliostat mirrors [3]. He concluded that the central receiver system provides a useful concentrator for solar thermal power generation, since a large amount of solar energy

can be concentrated and a temperature sufficient for Brayton as well as Rankine cycle operation is obtained very easily for such systems. Christian et al. presented a novel concept for a track-mounted heliostat intended to be manufacturable at low cost for central receiver CSP plants [5]. The cost can be reduced up to \$60/m<sup>2</sup> when implemented in high volume. An efficient autonomous solar energy system was implemented by Ali et al. which concentrates the solar heat to turn water into steam [6]. The prototype utilizes two heliostat reflectors which tracks the sun throughout the day and reflects the solar radiation constantly. The final system produced a concentration efficiency of 86% to 92%. Belaid et al. tried to optimize the solar tower power plant heliostat field by considering different heliostat shapes [7]. The results showed 69.65% increase in yearly efficiency for the case of the rectangular heliostat shape. Noone et al. introduced a biometric pattern for heliostat field layout and have done a detailed calculation of the annual average optical efficiency accounting various losses [8]. The calculations showed the improvement in PS10 field by 0.36% in efficiency while simultaneously reducing the land area by 15.8%. Kiwan et al. introduced and investigated a novel idea of using two receivers on the same tower in a solar tower system [9]. It was concluded that the annual weighted optical efficiency for the 50 MW plant for a single receiver is 67.14%, while it reaches 67.64% using the two-receiver system.

## 2 Objective

Several researchers have tried to optimize large-scale heliostat field by assuming the dimensions of heliostat reflectors. In several cases, the width of the heliostat reflector is assumed as 12.84 m while the height as 9.45 m [7–9] to get the field optimization of the heliostat solar reflector plant, but the physics behind the selection of that particular parameters was not available. Besides this, several techniques have been carried out to track the solar radiation by using different mechanisms in case of heliostat reflectors. Some researchers have even tried to optimize the geometrical parameters of heliostat numerically and experimentally by considering the concentration factors. But there are very few studies carried out which specifies the ideal geometrical configuration that maximizes the solar radiation. Information of such optimized topology may help in designing corresponding furnace which can cater commercial applications like baking, etc. the present work helps in arriving out such dimensionless geometrical configuration that ensures maximum solar radiation at the base collector.

## 3 Methodology

In the present work, a number of heliostat reflectors are arranged in a geometry which is made in the form of an inverted frustum of a square pyramid which accepts the radiation from the top and diverts it to a bottom collector by way of multiple reflections

on the different slanting side reflectors (refer Figs. 1 and 2). A dimensionless ratio of top and bottom side and ratio of bottom side to the height can be a representative ratio for optimization. This can be obtained by testing various sizes of reactor design and obtaining efficiency of the reflector in each case. Different configurations were considered for the present study, and for each design, the change in the reflector angle and base dimensions is systematically varied, and 32 such combinations of design are considered for testing. Each design is further tested for a span of operation starting from 9:00 to 17:00 h of the day, and collector efficiency is determined at a regular interval of 15 min; this makes 33 instances of operation for each design configuration in a day of operation. Use of CFD technique is chosen to carry out this large number of numerical experiments as a means of testing is carried out. In doing so, solar database of Ansys Fluent is considered as an input to the analysis.

To understand the working of the reflector, two extreme cases of the collectors are considered. One is with the base area of  $4.76 \times 4.76$  m, while another is with the base area of  $1 \times 1$  m. The area of the top reflector in each case is kept constant, i.e.,  $5 \times 5$  m and the height of the reflector is kept constant, i.e., 1.75 m. As shown in Fig. 1, a typical reflector can have three basic types of rays. Type A rays, which reach the base collectors via multiple reflections. Type B rays, which never reach the base, and Type C rays, which reach the base directly. Figure 2 shows the basic configuration of the reflectors, and here TS, BS, and H are three key dimensions which are top side, bottom side, and height of the reflector, respectively (refer Fig. 2). For a reflector design having a fixed value of TS and H when BS is very small, the ray type B will be in a large number compared to ray types A and B. This type of reflector design will have poor reflector efficiency. On the other hand, when difference between TS and BS will be small for a fixed value of H, ray type C will be in the large number compared to A and B.

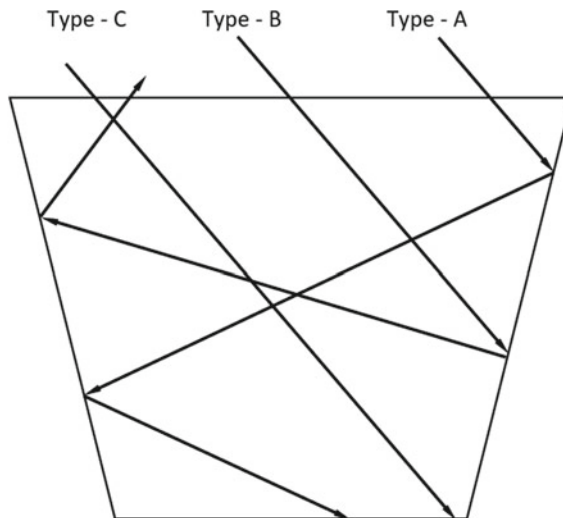


**Fig. 1** Different types of rays encountered by reflector

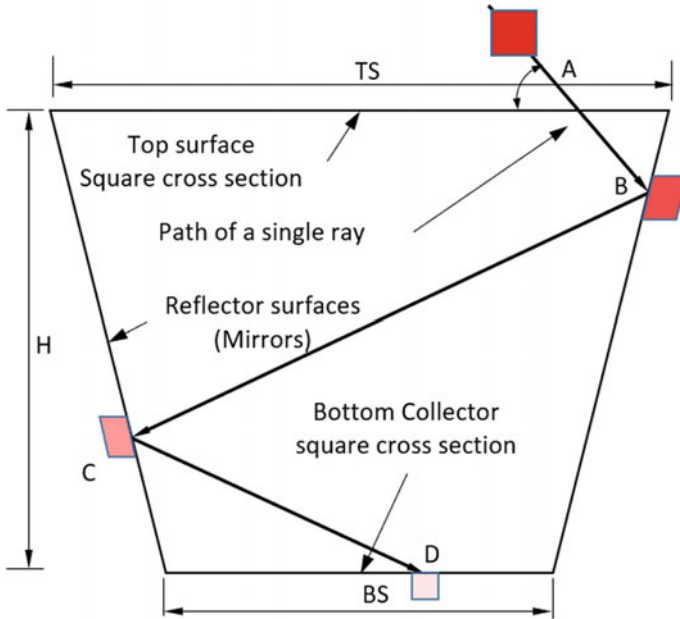


Fig. 2 Heliostat reflector configuration

## 4 Geometrical Modeling and Meshing

### 4.1 Geometrical Modeling

In order to find out an optimum ratio of  $BS/TS$ , when  $H$  is constant that will give maximum value of reflector efficiency, 33 different combinations of the geometric configuration of the reflector design are considered which is as shown in Fig. 4.

To carry out the CFD analysis of each configuration, geometry was created using ANSYS Space Claim as shown in Fig. 3. The geometry is created by keeping four reflectors side by side making a shape of an inverted frustum of a square pyramid. The thickness ( $t$ ) of the reflector is considered as 0.03 m. The thickness ( $t_b$ ) of the base collector is also kept 0.03 m. The height ( $h$ ) of the reflector is kept constant as 1.75 m for all design. The area of the top reflector is also kept constant and that is  $(A_t) 5 \times 5$  m. For the analysis, the area of the base ( $A_b$ ) is increased 5% in each step as shown in Fig. 4 to get the variation in the base length as well as reflector angle. This is done to find the best configuration for topology optimization. Totally, 33 geometric shapes were created which are as shown in Fig. 3 and meshed in Ansys Meshing module.

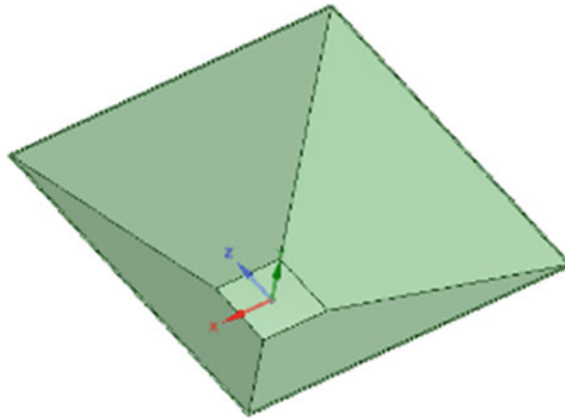


Fig. 3 Geometrical model for the analysis

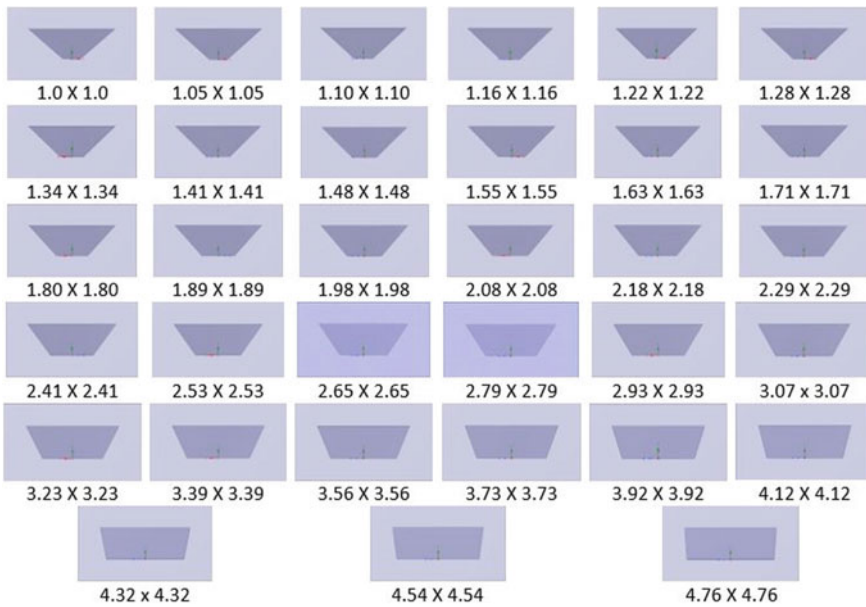


Fig. 4 Front view of geometry with variation at base

## 4.2 Meshing

In the present work, geometry was first split into different subvolumes to create meshing having uniform grid [10]. Meshing was carried out by edge sizing and face meshing operations. The mesh size near the reflectors and base plate is kept dense which was facilitated by giving biased edge sizing. This gives sufficient amount

of mesh elements near important geometrical features along with uniform mesh elements throughout the domain. The number of elements for the domain is 2,23,400. Figure 5 shows the meshing of the whole computational domain which was done using Ansys Meshing module. Figure 6 shows the cross-sectional view of the meshing at the center plane of the computational domain. As shown in Fig. 6, the meshing is denser at the base plate as well as the reflectors.

**Fig. 5:** 3D view of meshing for analysis

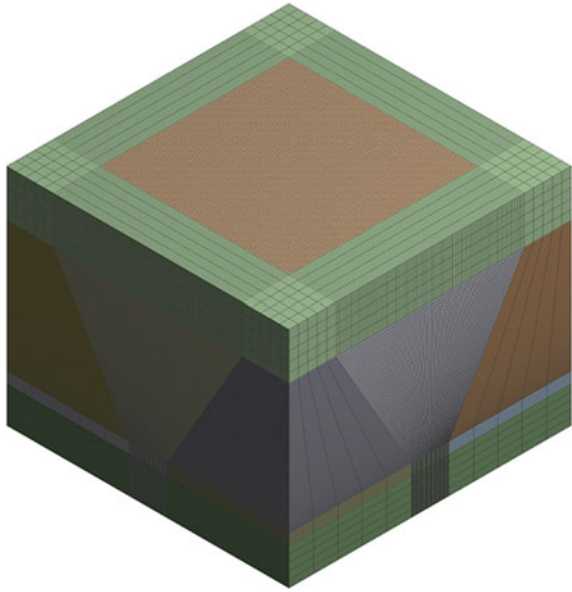


**Fig. 6** Front view of the meshing

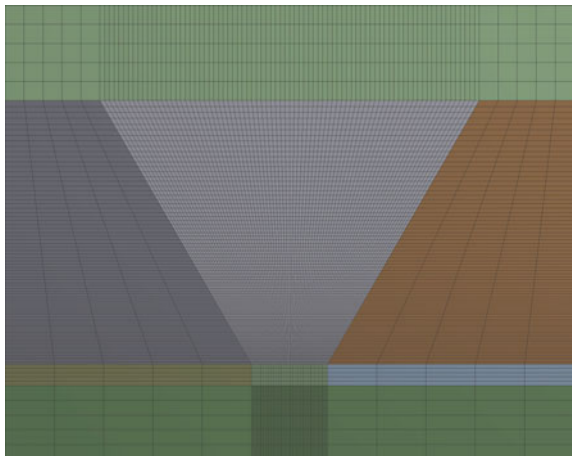


**Table 1** Properties of materials used

Material	$\rho$ (kg/m <sup>3</sup> )	$k$ (W/m <sup>2</sup> K)	$C_p$ (J/mK)
Mirror	2800	1.6	830
Glass	2500	1.15	830
Steel	8030	16.27	502.48

### 4.3 Boundary Conditions and Models Applied

Rossland with solar load model was selected as radiation model. As the intensity of the radiation changes with respect to time, transient solver with double precision is used. Also, radiation model supports only the pressure-based solver. For turbulence, standard  $k - \epsilon$  model is selected. Location of Pokhran situated in Rajasthan, India, with latitude of 26.92050 and longitude of 71.91650 is selected for the present study. For the analysis, the day of 21 May is selected. The results are generated from 9:00 h in the morning to 17:00 h in the evening with the interval of 15 min. Standard operating conditions of atmospheric pressure ( $p_{atm}$ ) as 1.01325 bar and atmospheric temperature ( $T_{atm}$ ) as 300 K are considered.

Mirror is used as the reflector material. The base was considered as steel. The material of the top surface is glass. The standard properties of the air are considered. The emissivity of mirror is taken as 0.03 which is opaque wall. The emissivity of steel is taken as 0.8 for opaque wall. The thickness of all the mirrors, glass, and base plate is taken as 0.003 m. The properties of all the materials used are shown in Table 1.

## 5 Results and Discussions

CFD analysis is carried out for a selected particular day, time, and place. In the present case, the day considered is 21 May. This day is considered since it is the hottest day in the year compared to other days in summer season. The period of operation considered for analysis is from 0900 to 1700 h. The analysis is carried out for the interval of 15 min. The purpose of considering this time zone for the analysis is that beyond this time zone, the radiation intensity is found to be negligible. Since Rajasthan is having very high intensity of radiation density and clear weather, one of the locations of Rajasthan, i.e., Pokhran is considered for the analysis. The analysis considers the convection heat loss from the bottom reflector and the heat absorbed at the reflector surfaces which are two important factors for the analysis. Additionally, the emissivity of the reflector is considered as 0.03, which is in line with the reflectivity of a high-quality mirror available in the market.

In the present analysis, the time for the solar calculator available in the Ansys Fluent database is changed manually for each increment. This will help consider the direct irradiation and diffuse irradiation values into the calculations directly by using



an inbuilt solar calculator provided in the Ansys Fluent application. Both the direct and diffuse irradiation may be changed by just changing the time of the day. Also, this value changes by changing the place and date. Result of analysis is generated in terms of temperature contours taken at interval of 1 h each, taking radiation heat flux value at top and base of the reflector from Fluent (average value) and plotting graph of radiation heat flux at base ( $\text{W/m}^2\text{-day}$ ) vs. radiation heat flux at top ( $\text{W/m}^2\text{-day}$ ).

As shown in graph above in Fig. 7, the first point considered on the extreme right of the graph has coordinates as 3877.08 and 8742.28  $\text{W/m}^2\text{-day}$ . In order to vary the angle, the base length of reflector is increased in step. It is observed from Fig. 7 that with each increase in the base length, the net radiation heat flux received at the top surface decreases while the net radiation heat flux received at the base increases. This trend is continued until a point where net radiation at the bottom of reflector is maximum. The 20th design combination gives this condition (refer Fig. 4). Beyond this point, all further design consideration that will reduce the net total radiation received at the base collector shows that the concentration of rays is increasing up to optimum point, 20th design point in this case, and then the concentration of rays decreases. On further increasing the base area from optimum point, the rate of decreasing of heat flux at base increases which shows that the role of reflector, i.e., reflection by reflector decreases. And at one point, the value of heat flux at top is almost equal to heat flux at base. To get the maximum solar radiation of the bottom, a concentration factor is defined which will give the improvement made by varying the geometrical parameters of the reflectors. In Sect. 3, it was discussed that there is a direct effect of the geometry which causes the concentration of the maximum solar radiation at the bottom. As we move toward the optimum point in the graph, the concentration at the bottom increases due to the dominant effect of type A and type C rays.

$$\text{Concentration Factor} = \frac{\text{Radiative Heat Flux at bottom}}{\text{Radiative Heat Flux at top}} \quad (1)$$

It is obvious that the relative ratio of types A, B or C of rays will vary throughout the operation of the day for a given location of site on the earth. Additionally, this distribution will also depend on the physical location of the operation of the site of the solar system, i.e., its latitude and longitude. As the combination of types A, B and C at a given instance of time will be different at different latitude of the earth. For instance, contribution of ray type C will be more for a given design of reflector operating at equator; however, if the same reflector design is made to operate at say  $45^\circ$  latitude, some of the ray type C will be converted to ray types A and B. The corresponding reflector efficiency will also be different in both the cases. Although, the effect of the location will be a factor on the operation and optimum design of the solar reflector.

Figure 8 represents the temperature distribution over the reflectors and base plate in case of an optimum angle geometry design. In this it can clearly be seen that with change in the sun's position, the left vertical slanting reflector surface is gradually showing higher and higher temperature. The trend is continued until 1300 h after this

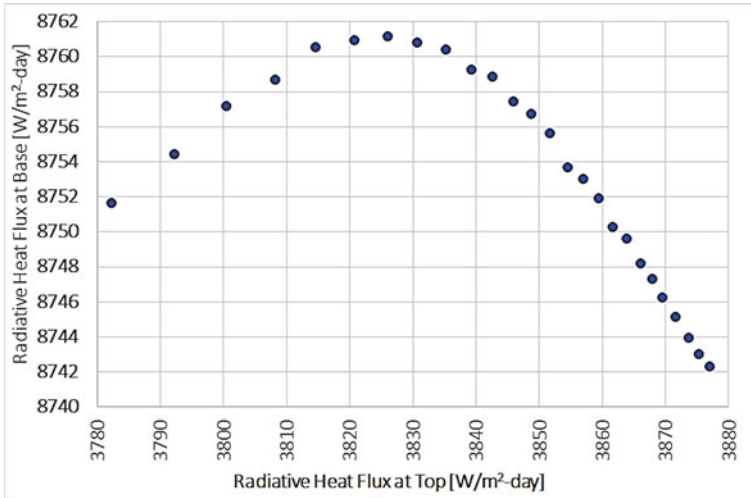


Fig. 7 Radiation heat flux at base versus top

gradual decrease in the temperature is observed. One can see clear transition in the temperature with passage of time. It is important to note that a little in-depth analysis of the reflector temperature with time will reveal clearly that the site selected for the analysis is not located at the equator but has certain angle of latitude, and the path of the sun is not exactly above the reflector.

Other observation made is that the maximum heat flux at the base was achieved in a day at 1545 h in case of the Rajasthan, Pokhran. However, carrying out similar analysis in case of Chennai, the maximum heat flux condition is observed at 1530 h

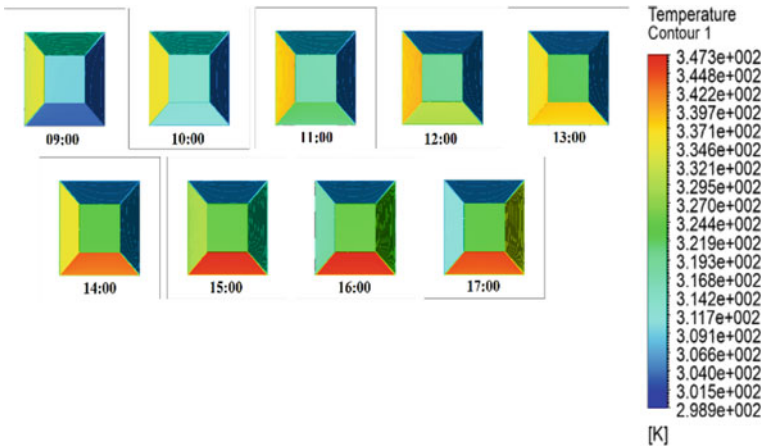


Fig. 8 Temperature contour for reflector at different time of the day

only. Above observation confirms the influence of the location of operation of the reflector on the efficiency of the reflector. In the present case, it was observed that the value of heat flux depends upon the position with reference to Tropic of Cancer, Equator, and Tropic of Capricorn. As the present study is carried out in India, one can say, based on the two extreme locations, that all over India the maximum radiation heat flux may occur between 1530 (for South India) and 1545 (for North India). The influence of finding the optimum angle for a particular type of reflector by changing the position is matter of further investigation.

This fact can be observed based on the Fig. 9. Figure shows the variation in the concentration factor between bottom reflector heat flux density and the top reflector heat flux density when size of bottom side of the reflector considered is  $1 \times 1$  m. The three cities across the latitude of the India are considered, and they are Chennai in state of Tamil Nadu, Pokhran in the state of Rajasthan, and Meerut in the state of Uttar Pradesh. Based on the day chosen in the analysis which is 21 May, one can say that the tilting of northern hemisphere will be toward the sun as shown in the inset figure in Fig. 9. It is observed that due to the tilting, Pokhran will be the nearest city to the sun followed by Chennai and lastly Meerut. This is obvious from the concentration ratio also. It is observed that there is not only variation in the concentration factor but also the timing in which the peak of the concentration factor occurs. In case of Pokhran, the peak is achieved almost at the same time, i.e., at 15:30 h, compared to Chennai. It is important to note that due to the variation in latitudes of the respective locations, the variation in the combination of the rays (A, B or C) is observed. This variation is reflected in the concentration factor also. The variation may explain the existence of variation in distribution of types A, B, or C rays and their relative distribution due to the position of the reflector on the earth.

## 6 Conclusions

The study proposes the best configuration of reflector design. The analysis is carried out for time interval of 15 min each through the active time span of the day (from 9 AM to 5 PM) of the solar path. The radiation data considered for Pokhran, Rajasthan, India (latitude 26.92050 and longitude 71.91650). The temperature contours discussed can be helpful in the future works to identify and improve the reflector design. The design optimization can be further improved by varying the reflectivity of the mirrors as we know that as we move from bottom to top, the role of a reflector to concentrate the solar radiation decreases.

Based on the optimum condition, the study proposes two dimensionless numbers: (a) reduction ratio and (b) height to base width, the value of both is 2 and 0.7, respectively. The description of these number is as follows. The results derived in the present studies matches the dimensions considered by the researcher in the previous studies [7–9].

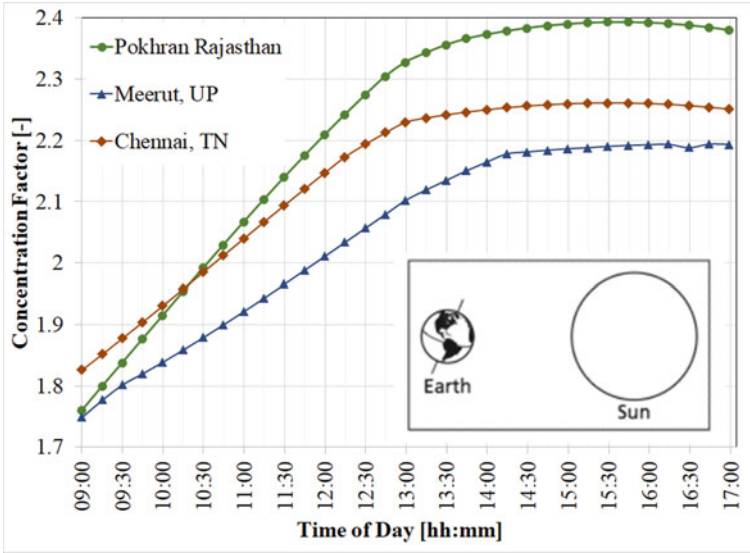


Fig. 9 Variation in concentration factor with time for different cities of India

$$\begin{aligned}
 \text{Height to base width} &= \frac{\text{Height of the reflector } (H)}{\text{Width of the base } (BS)} \\
 &= 0.7
 \end{aligned}
 \tag{2}$$

$$\begin{aligned}
 \text{Reduction Ratio} &= \frac{\text{Width at the top } (TS)}{\text{Width at the bottom } (BS)} \\
 &\approx 2
 \end{aligned}
 \tag{3}$$

The result is useful for large applications, for which the tracking of solar reflectors is not a practical option, and this is due to a large inertia of the reflectors. Under this, a particular design of the reflectors is standardized and tested to obtain the maximum radiation at the bottom plate that will help bypass the need of tracking. It appears that there is very small variation in the concentration factor values for different cities in India. Therefore, one can use a standard design of reflector for all the cities of India with very less variation.

## References

1. Ernst, Young (2021) “2021 Renewable energy country attractiveness index (RECAI)”. ([https://www.ey.com/en\\_sg/recai](https://www.ey.com/en_sg/recai))
2. “Brighter days await renewable energy space; investments likely to cross \$15 billion in 2022”, The Hindu. PTI, ISSN 00971-751X (<https://www.worldcat.org/issn/0971-751X>) December 24, (2021)
3. Sakurai T, Shibata Y (1982) Theoretical concentration of solar radiation by central receiver systems. *Solar Energy* 31(3):261-270
4. Riaz MR (1976) A theory of concentrators of solar energy on a central receiver for electric power generation. *ASME J Eng Power*
5. Davila-Peralta C, Rademacher M, Emerson N, Lopez GC, Sosa P, Cabanillas R, Peon-Anaya R, Montijo NF, Didato N, Angel R (2020) Progress in track-mounted heliostat, AIP Publishing, AIP Conference Proceedings 2303, 030011, December 11
6. Ali NT, Mezher KA, Qayed AA, McEwan N, AlTimimi AMM (2012) Efficient autonomous heliostat system. In: 2012 16th IEEE Mediterranean electrotechnical conference, IEEE, pp 573-576
7. Belaid A, Filai A, Gama A, Bezza B, Arrif T, Bouakba M (2022) Design optimization of a solar tower power plant heliostat field by considering different heliostat shapes. *Int J Energy Res* 1-18
8. Noone CJ, Torrilhon M, Mitos A (2012) Heliostat fields optimization: a new computationally efficient model and biomimetic layout. *Solar Energy* 86:792-803
9. Kiwan S, Khammash AL (2020) Optical performance of a novel two-receiver solar central tower system. *J Solar Energy Eng* 142:011005-1
10. Jayesh B, Kevat MD, Patel AR (2022) CFD analysis of air inside a circular duct around a series of vertically heated circular baffled discs at a different angles. In: 20th ISME conference on advances in mechanical engineering, May 2022, Ropar, Punjab